

ARTICLE

# Natural radioactivity measurements and external dose estimation by car-borne survey in Douala city, Cameroon

S.D. Takoukam Soh<sup>1,2</sup>, Saïdou<sup>1,2,\*</sup>, M. Hosoda<sup>3</sup>, J.E. Ndjana Nkoulou II<sup>2</sup>, N. Akata<sup>4</sup>, O. Bouba<sup>1</sup> and S. Tokonami<sup>5</sup>

<sup>1</sup> Nuclear Physics Laboratory, Faculty of Science, University of Yaoundé I, P.O. Box 812 Yaoundé, Cameroon.

<sup>2</sup> Nuclear Technology Section, Institute of Geological and Mining Research, P.O. Box 4110 Yaoundé, Cameroon.

<sup>3</sup> Hirosaki University Graduate School of Health Sciences, Hirosaki City, Aoromi, Japan.

<sup>4</sup> National Institute for Fusion Science, 322-6 Oroshi, Toki, Gifu 509-5292, Japan.

<sup>5</sup> Department of Radiation Physics, Institute of Radiation Emergency Medicine, Hirosaki University, Hirosaki City, Aomori 036-8564, Japan.

Received: 23 January 2018 / Accepted: 27 July 2018

**Abstract** – A car-borne survey was carried out in Douala, the largest city in Cameroon to make a detailed distribution map of the absorbed dose rate in the city, to locate the high natural radiation areas useful later to carry out indoor radon, thoron, and thoron progeny measurements. Gamma-ray dose rates were measured using 3-in × 3-in NaI(Tl) detector. Activity concentrations of <sup>238</sup>U, <sup>232</sup>Th and <sup>40</sup>K in soil from Douala city were determined by two methods: the first, using *in situ* gamma spectrometry and the second, at the laboratory using a NaI(Tl) detector. A heterogeneous distribution of absorbed dose rates in air was observed on the dose rate distribution map, and varies from 29 to 86 nGy h<sup>-1</sup> with an average of 50 nGy h<sup>-1</sup>, lower than the world average value of 59 nGy h<sup>-1</sup>. The activity concentrations with NaI(Tl) detector varied from 18 to 47 Bq kg<sup>-1</sup> for <sup>238</sup>U, 21 to 54 Bq kg<sup>-1</sup> for <sup>232</sup>Th, and 10 to 410 Bq kg<sup>-1</sup> for <sup>40</sup>K with averages of 29, 38, and 202 Bq kg<sup>-1</sup> respectively, for *in situ* measurements. They vary between 29–98 Bq kg<sup>-1</sup> for <sup>238</sup>U, 29–92 Bq kg<sup>-1</sup> for <sup>232</sup>Th, and 40 to 79 Bq kg<sup>-1</sup> for <sup>40</sup>K, with averages of 60, 57, and 56 Bq kg<sup>-1</sup> respectively for soil samples collected at Douala III subdivision. The highest value of the annual effective dose for *in situ* measurements by car was observed at Ndogbong and was found to be 0.7 mSv y<sup>-1</sup>, higher than the world average value of 0.5 mSv y<sup>-1</sup>.

**Keywords:** car-borne survey / NaI(Tl) detector / natural radioactivity / air absorbed dose rate / external effective dose

## 1 Introduction

Exposure to natural radiation sources varies substantially from one area to another and even locally (UNSCEAR, 1982). Gamma radiation from natural radionuclides such as <sup>238</sup>U, <sup>232</sup>Th and <sup>40</sup>K is the main source of external exposure. There are three sources of environmental radioactivity: terrestrial, manmade and cosmic. The most significant terrestrial radionuclides include the uranium and thorium decay series, potassium and rubidium (EPA, 2009). The terrestrial component is due to the radioactive nuclides that are present in air, soil, rocks, water and building materials whose amounts vary significantly depending on the geological and geographical features of the regions. Cosmic radiation from space contributes to the background changes chiefly through elevation and latitude (UNSCEAR, 2000).

Although background radiation is present everywhere, radionuclide concentrations and distributions are not constant (EPA, 2009). For ages, humans have been exposed to radionuclides that occur naturally in the environment. It is therefore important to measure the activity concentrations of radionuclides in the living environment.

There have been many surveys to measure natural radioactivity and to estimate corresponding radiation dose to the public in Cameroon. According to Guembou *et al.* (2017), absorbed dose rates and annual effective dose due to radioactivity in sand used as building material in Douala, were normal and within the recommended limits. Also, Saïdou *et al.* (2015a, 2015b) reported no significant radiological risk to population living in the oil-bearing Bakassi peninsula, in the uranium-bearing regions of Poli and Lolodorf. The average total radiation dose and external radiation dose were respectively 5.9 and 0.6 mSv y<sup>-1</sup> for Poli, 7.6 and 0.7 mSv y<sup>-1</sup> for Lolodorf, and 22.3 and 0.3 mSv y<sup>-1</sup> for Bakassi.

\*Corresponding author: [saidous2002@yahoo.fr](mailto:saidous2002@yahoo.fr)

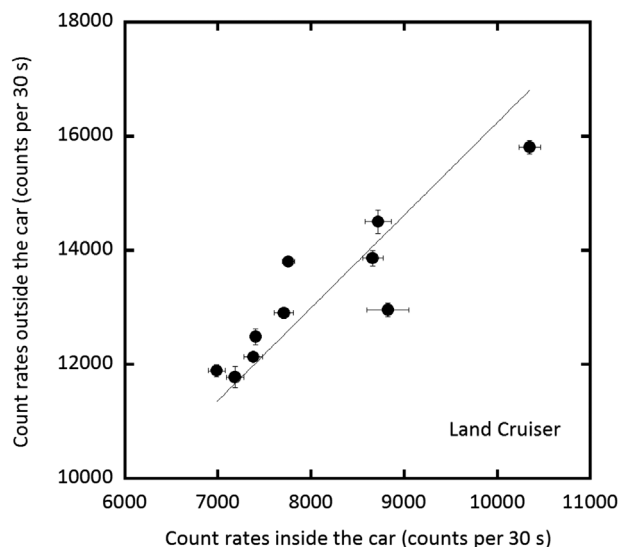


**Fig. 1.** Correlation between count rates outside and inside the car. This regression formula was used as the shielding factor of the car body.

In this study, a car-borne survey was carried out to establish the dose rate distribution map, to assess the annual external dose and to perform natural radioactivity measurements in soil from Douala, the largest city in Cameroon. Gamma ray spectrometry based on NaI(Tl) detector was also used in the laboratory to determine activity concentrations of  $^{238}\text{U}$ ,  $^{232}\text{Th}$  and  $^{40}\text{K}$  in soil.

## 2 Material and methods

### 2.1 Survey area

Douala is a coastal city, the economic capital of Cameroon, the main business center and the largest city of the country; with approximately 4 million inhabitants. It is the chief town of the Littoral Region and the Wouri Division. Located on the edge of the Atlantic Ocean, at the bottom of the Gulf of Guinea, at the mouth of the Wouri River, Douala has the largest port in the Cameroon and one of the most important in Central Africa. The annual rainfall ranges between 3000 and 5000 mm, and the annual average temperature is  $26^{\circ}\text{C}$  (Olivry, 1986). The geology of the region consists of sedimentary rocks, mainly, tertiary and quaternary sediments (Ndontchueng *et al.*, 2014).

### 2.2 Car-borne survey

A car-borne survey was carried out using a mobile vehicle moving at a speed of approximately  $40\text{ km h}^{-1}$ , in which was positioned a measuring system consisting of a sodium iodide detector 3-in  $\times$  3-in NaI(Tl), a global positioning system (GPS) to record coordinates at each measuring point, and a computer to analyze gamma-ray spectra (EMF-211, EMF Japan Co, Japan). Absorbed dose rate measurements inside the vehicle were performed every 30 seconds along the way and corrected by multiplying with a shielding factor with the aim of representing the

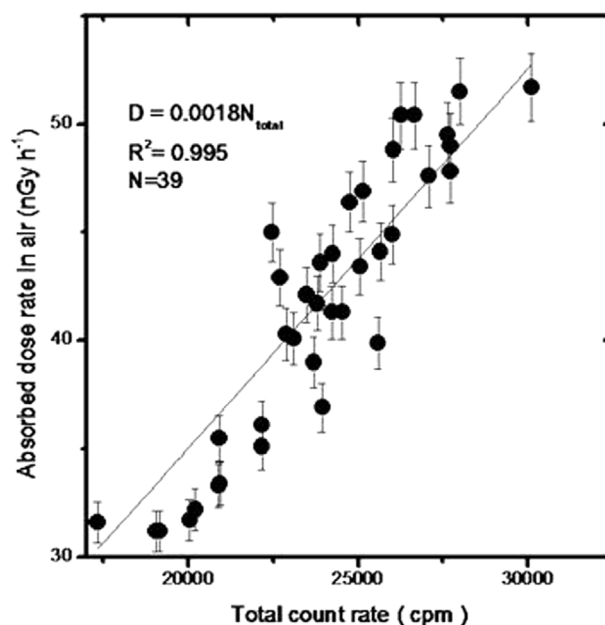


**Fig. 2.** Correlation between absorbed dose rate in air which was calculated by software using the response matrix method and total count rate observed outside the car. This regression formula was used as the dose rate conversion factor.

unshielded external dose rate. The shielding factor (Fig. 1) was evaluated in order to be able to convert the values measured inside the vehicle to ambient dose rate outside of the car, and was estimated by making measurements inside and outside the vehicle at 10 measurement points and correcting them with count rates inside. The absorbed dose rates in air were calculated using a dose rate conversion factor based on the correlation of dose rate ( $\text{nGy h}^{-1}$ ) and total count rate (cpm) from 0 to 1023 channels in the gamma-ray pulse height distribution (Hosoda *et al.*, 2015, 2016). Commonly, the gamma-ray pulse height distribution is obtained by 15 min measurements at each point. Measurements of gamma-ray pulse height distributions were carried out at 1 m above the ground surface at 39 measurement points in Douala City. The gamma-ray pulse height distributions were unfolded using a  $22 \times 22$  response matrix for the estimation of absorbed dose rate in air (Minato and Kawano, 1970; Minato, 2001). The dose rate conversion factor of the scintillation spectrometer used in the present survey was determined to be  $1.75 \times 10^{-3}\text{ nGy h}^{-1}\cdot\text{cpm}^{-1}$ . Figure 2 gives the relationship between absorbed dose rate ( $\text{nGy h}^{-1}$ ) which was calculated by software using the response matrix method and total count rates outside the vehicle. Absorbed dose rate in air ( $D_{out}$ ) 1 m above the ground surface at each measurement point can be estimated by the following equation (Tan *et al.*, 2017):

$$D_{out} = 2D_{in} \times (1.62) \times 0.00175, \quad (1)$$

where ( $D_{in}$ ) is the count rate inside the car (cps) obtained by the measurements for 30 seconds. Since the dose rate conversion factor was given as a dose rate ( $\text{nGy h}^{-1}$ ) for counts per minute (cpm), it is necessary to double  $D_{in}$  in order to convert into the counts per minute.

Following *in situ* measurements, external effective dose in Douala was assessed using the following equation (Inoue *et al.*, 2017):

$$E = D_{out} \times DCF \times T \times (Q_{in} \times R + Q_{out}) \times 10^{-6}, \quad (2)$$

where  $E$  is the external effective dose ( $\text{mSv y}^{-1}$ ),  $D_{out}$  is the absorbed dose rate in air ( $\text{nGy h}^{-1}$ ),  $DCF$  is the dose conversion factor from the dose rate to the external effective dose for adults ( $0.748 \pm 0.007 \text{ Sv Gy}^{-1}$ ) (Moriuchi *et al.*, 1990),  $T$  is 8766 h, and  $Q_{in}$  and  $Q_{out}$  are indoor (0.6) and outdoor (0.4) occupancy factor respectively.  $R$  (1.11) is the ratio of indoor and outdoor dose rate.

### 2.3 Activity concentrations of $^{238}\text{U}$ , $^{232}\text{Th}$ and $^{40}\text{K}$ and their contribution to the air absorbed dose rate

The evaluation of activity concentrations and the contribution of  $^{238}\text{U}$ ,  $^{232}\text{Th}$  and  $^{40}\text{K}$  to the absorbed dose rate in air were obtained by measuring the spectra of gamma-ray pulse height distributions and using a  $22 \times 22$  response matrix conceived by Minato (1978, 2001). The gamma-ray pulse height distribution obtained by measurements was converted to the energy bin spectrum of incident gamma-ray which is a distribution of gamma-ray flux density to each energy bin. The energy ranges from 0 to 3.2 MeV, energies above 3.2 MeV were not included for evaluation because the maximum value of the gamma-ray energy from natural radionuclides is 2.615 MeV emitted by  $^{208}\text{Tl}$  ( $^{232}\text{Th}$ -series). The gamma-ray lines utilized for natural radionuclides are: 1.464 MeV for  $^{40}\text{K}$ , 1.768 MeV and 2.205 MeV for  $^{214}\text{Bi}$  ( $^{238}\text{U}$ -series), and also 2.615 MeV for  $^{208}\text{Tl}$  ( $^{232}\text{Th}$ -series). The  $22 \times 22$  matrix for the 3-in  $\times$  3-in NaI(Tl) scintillator for an isotropic field was calculated using the Monte Carlo code, SPHERIX (Matsuda *et al.*, 1982; Minato, 2012). The gamma-ray flux density and dose rate per unit solid angle are considered almost isotropic in the natural environment (Minato, 1971). The calculation of gamma-ray flux densities per unit activity concentrations of  $^{238}\text{U}$ -series,  $^{232}\text{Th}$ -series and  $^{40}\text{K}$  are necessary, in order to evaluate each activity concentrations of natural radionuclides from an energy bin spectrum. This calculation assumed that a semi-infinite volume source was formed in the ground (Minato, 2001). The primary and scattered gamma-ray flux density per unit activity concentrations could be calculated using one-dimensional Monte Carlo gamma transport code, MONARIZA/G2 (Minato, 1977, 1980). A total of a million histories were traced for each natural radionuclide. The nuclear data of gamma-ray energies and disintegration rates used the reported values by Beck (1972) and Beck *et al.* (1972) for this Monte Carlo simulation. The activity concentration of each natural radionuclide was evaluated by a successive approximation which used a  $3 \times 3$  matrix, determined by Minato (2001), to the values of energy bins for  $^{238}\text{U}$ -series,  $^{232}\text{Th}$ -series and  $^{40}\text{K}$ . The statistical errors for absorbed dose rates in air and activity concentrations for  $^{40}\text{K}$ ,  $^{238}\text{U}$ -series and  $^{232}\text{Th}$ -series obtained using this software depend on the integral air kerma ( $\text{nGy h}^{-1}$ ) at each measurement point (Matsuda *et al.*, 2002), and these were evaluated in this study as 2%, 2%, 6–8% and 4–5%, respectively.

### 2.4 Sampling and sample preparation

For radioactivity measurements in soil, twenty soil samples from a depth of 0–5 cm, weighing about 1 kg each were collected at Douala III, pulverized and then dried at a temperature of 70 °C for 48 hours to remove moisture. Samples were then transferred to Marinelli containers of 500  $\text{cm}^3$ , each hermetically sealed and stored for more than 40 days to bring  $^{222}\text{Rn}$  and its short-lived daughter products into equilibrium with  $^{226}\text{Ra}$  (Ravisankar *et al.*, 2011).

### 2.5 Radioactivity measurements in laboratory

$^{238}\text{U}$ ,  $^{232}\text{Th}$  and  $^{40}\text{K}$  activity concentrations in soil samples were measured using a gamma ray spectrometer. The samples were placed in a shielded gamma ray spectrometry unit for a counting time of  $10^5$  seconds. Radioactivity measurements were carried out using a NaI(Tl) detector of 7.6 cm  $\times$  7.6 cm size and a resolution of 7.5% at 661.6 keV with a 1024 channels multichannel analyzer. The detector was calibrated using the standard gamma ray source of  $^{137}\text{Cs}$  with known peak at 661.6 keV,  $^{152}\text{Eu}$  with known peaks at 1089.7 keV, and 1408.1 keV and  $^{60}\text{Co}$  with known peaks at 1173.2 keV and 1332.5 keV. The efficiency calibration curve for NaI(Tl) detector was obtained using standards containing  $^{40}\text{K}$  (1460.8 keV),  $^{137}\text{Cs}$  (661.6 keV),  $^{208}\text{Tl}$  (2614.4 keV) and  $^{228}\text{Ac}$  (940.1 keV). Gamma-ray lines of  $^{214}\text{Bi}$  were used to determine  $^{238}\text{U}$  activity concentrations after reaching secular equilibrium between  $^{222}\text{Rn}$  and its daughter products  $^{214}\text{Bi}$  and  $^{214}\text{Pb}$ . Gamma-ray lines of  $^{228}\text{Ac}$  were considered to determine activity concentrations of  $^{232}\text{Th}$ .

The spectral analysis was performed using Genie-2000. Activity concentrations of natural radionuclides in samples were computed using the following equation (IAEA, 1989):

$$A = \frac{N_p}{t_c I_\gamma(E_\gamma) \epsilon(E_\gamma) M}, \quad (3)$$

where  $N_p$  is the number of counts in a given peak area corrected for background peaks of a peak at energy  $E$ ,  $\epsilon(E_\gamma)$  the detection efficiency at energy  $E$ ,  $t_c$  is the counting lifetime,  $I_\gamma(E_\gamma)$  is the number of gamma rays per disintegration of this nuclide at energy  $E$ , and  $M$  the mass in kg of the sample.

### 2.6 Estimation of absorbed dose rate in air and external effective dose

The external terrestrial gamma-radiation absorbed dose rates in air at a height of about 1 m above the ground are calculated by using the conversion factor  $0.0417 \text{ (nGy h}^{-1}\text{)} (\text{Bq kg}^{-1})^{-1}$  for  $^{40}\text{K}$ ,  $0.462 \text{ (nGy h}^{-1}\text{)} (\text{Bq kg}^{-1})^{-1}$  for  $^{238}\text{U}$  and  $0.604 \text{ (nGy h}^{-1}\text{)} (\text{Bq kg}^{-1})^{-1}$  for  $^{232}\text{Th}$  (UNSCEAR, 2000). Assuming that,  $^{137}\text{Cs}$ ,  $^{90}\text{Sr}$  and the  $^{235}\text{U}$  decay series can be neglected as they contribute very little to the total dose from the environmental background (Kocher and Sjoreen, 1985; Jacob *et al.*, 1986; Leung *et al.*, 1990):

$$D(\text{nGy h}^{-1}) = 0.462A_U + 0.604A_{Th} + 0.0417A_K, \quad (4)$$

where  $A_U$ ,  $A_{Th}$  and  $A_K$  are the mean activity concentrations of  $^{238}\text{U}$ ,  $^{232}\text{Th}$  and  $^{40}\text{K}$ , respectively in ( $\text{Bq kg}^{-1}$ ).

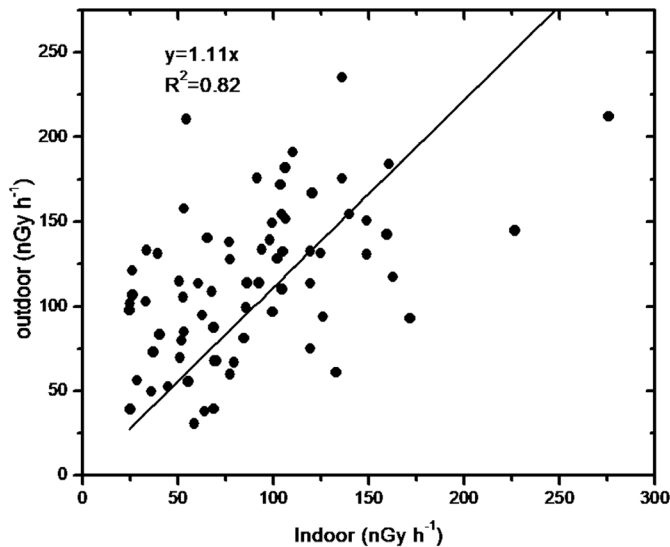


Fig. 3. Correlation between outdoor and indoor dose obtained by car-borne survey in Douala rate.

In the estimation of external effective dose, the conversion coefficient and occupancy factor must be taken into account. In the present work, a conversion factor of  $0.7 \text{ Sv Gy}^{-1}$  and occupancy factors  $Q$  have been used to convert the absorbed rate to human effective dose equivalent with an outdoor and indoor occupancy of 40% and 60% respectively. However, since the materials used in the construction of most these buildings also contain radionuclides,  $R$  (1.11) is the ratio of indoor and outdoor dose rate (Fig. 3). It should be noted that the dwellings were built mainly using locally made soil bricks.  $A_i$  are average activity concentrations of  $^{238}\text{U}$ ,  $^{232}\text{Th}$  and  $^{40}\text{K}$ .  $(KCF)_i$  are corresponding air kerma conversion factors given previously. The external effective dose is determined as follows (Saïdou *et al.*, 2015b):

$$E_{ext}(\text{mSv y}^{-1}) = F_C \times [Q_{in} \times R + Q_{out}] \sum_{i=1}^3 A_i (KCF)_i \times t. \quad (5)$$

## 3 Results and discussion

### 3.1 Shielding factor and dose rate conversion factor

The relationship between count rates inside and outside the car is shown in Figure 1, and the shielding factor and standard uncertainty (JCGM 100, 2008) were found to be 1.62 and 0.03, respectively. However, the shielding factor is influenced by the type of car, number of passengers and detector position inside the car.

Figure 2 shows the correlation between absorbed dose rates in air ( $\text{nGy h}^{-1}$ ) calculated using the  $22 \times 22$  response matrix method and count rate outside the car (cps) (that is corrected count rate inside the car). The dose conversion factor and uncertainty were found to be  $0.00175 \text{ nGy h}^{-1} \text{ cps}^{-1}$  and 0.01, respectively (Fig. 2). Thus, the absorbed dose rate in air ( $D_{out}$ ) outside the car 1 m above the ground surface at each measuring

point can be estimated using the following equation (Tan *et al.*, 2017):

$$D_{out} = 2D_{in} \times 1.62 \times 0.00175, \quad (6)$$

where ( $D_{in}$ ) is count rate inside the car (cps) obtained by measurements for 30 seconds.

### 3.2 Air absorbed dose rate distribution in Douala city and effective external dose

Figure 4 shows the survey route and Figures 5 and 6 show the measurement points of gamma-ray pulse height distribution of Douala. The highest air absorbed dose rates ( $86 \text{ nGy h}^{-1}$ ) were observed at Ndogbong (N4.058778, E9.74635). The absorbed dose rates in this study range between  $28\text{--}86 \text{ nGy h}^{-1}$  with the average value of  $50 \text{ nGy h}^{-1}$  (Fig. 7). According to UNSCEAR (2000) at worldwide level, gamma dose rates in air range between  $24\text{--}160 \text{ nGy h}^{-1}$  and the average is  $59 \text{ nGy h}^{-1}$ , higher than the average value obtained within the framework of this study. However at Ndogbong, Aeroport, Ndogpassi III, Bepanda Omnisports, and Brazzaville, air absorbed dose rates are higher than the worldwide average value. The town of Kerala in India recorded large values of the absorbed dose rate, up to  $2100 \text{ nGy h}^{-1}$ , observed near the rare earth mining (Hosoda *et al.*, 2015). In Tokyo, air absorbed dose rates range from  $18$  to  $76 \text{ nGy h}^{-1}$  with an average value of  $49 \text{ nGy h}^{-1}$  (Inoue *et al.*, 2015), and from  $9$  to  $554 \text{ nGy h}^{-1}$  with an average value of  $50 \text{ nGy h}^{-1}$  in Turkey (Turhan *et al.*, 2012), which is practically lower than the corresponding worldwide value.

### 3.3 Effective dose assessment

The external annual effective dose ranged from  $0.21$  to  $0.41 \text{ mSv y}^{-1}$  with a mean value of  $0.31 \text{ mSv y}^{-1}$ , less than the worldwide average value of  $0.5 \text{ mSv y}^{-1}$  (UNSCEAR, 2000). In the Gold Mining Areas of Betare-Oya, Eastern-Cameroon, the mean value of effective dose is  $0.33 \text{ mSv y}^{-1}$  ( $0.17\text{--}0.60 \text{ mSv y}^{-1}$ ) (Ngoa *et al.*, 2017) and in Tokyo, before the Fukushima Daiichi Nuclear Power plant Accident, the arithmetic annual effective dose was  $0.32 \text{ mSv y}^{-1}$  ( $0.26\text{--}0.40 \text{ mSv y}^{-1}$ ) (Inoue *et al.*, 2015), which are practically lower than the corresponding worldwide value.

### 3.4 *In situ* activity concentrations of $^{238}\text{U}$ , $^{232}\text{Th}$ and $^{40}\text{K}$ and their contribution to air absorbed dose rate

According to Table 1, activity concentrations for primordial radionuclides range between  $18\text{--}47 \text{ Bq kg}^{-1}$ ,  $21\text{--}54 \text{ Bq kg}^{-1}$  and  $110\text{--}410 \text{ Bq kg}^{-1}$  for the  $^{238}\text{U}$  series,  $^{232}\text{Th}$  series and  $^{40}\text{K}$  respectively, with corresponding average values of  $29 \text{ Bq kg}^{-1}$ ,  $38 \text{ Bq kg}^{-1}$  and  $202 \text{ Bq kg}^{-1}$ . For  $^{238}\text{U}$  and  $^{232}\text{Th}$ , 7/39 and 32/39 measurement points have respectively activity concentrations higher than the world average value (UNSCEAR, 2000). For  $^{40}\text{K}$ , 1/39 measurement point has activity concentrations higher than the world average. By comparing the average *in situ* activity concentrations of  $^{238}\text{U}$ ,  $^{232}\text{Th}$  and  $^{40}\text{K}$  in Douala with the average values in other areas of Cameroon and other countries as shown in Table 3, it should be noted that the

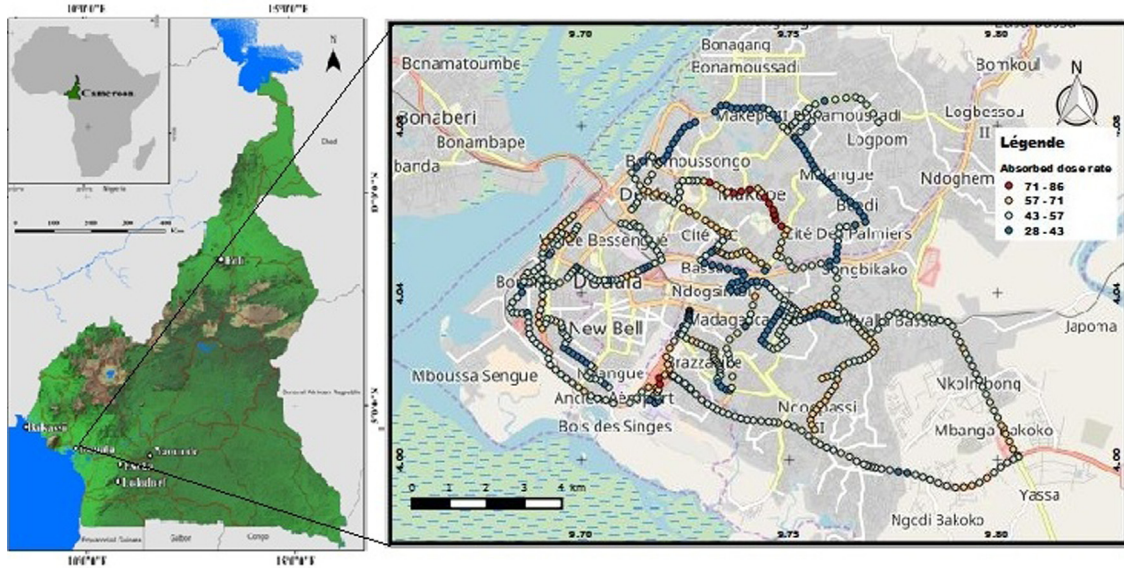


Fig. 4. Survey route in Douala. This map was also drawn using QGIS (Background: Openstreet map).

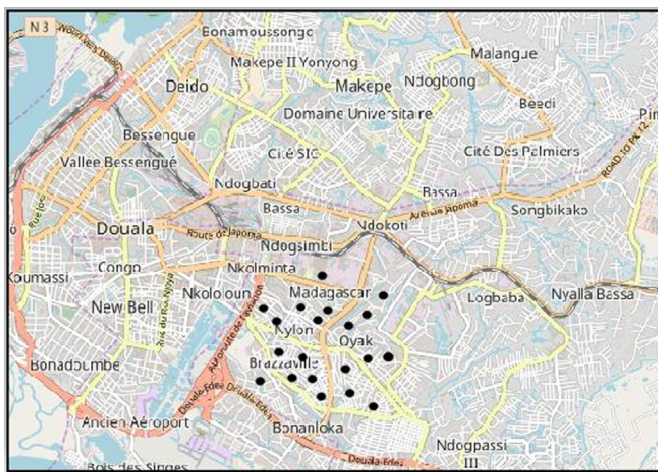


Fig. 5. Location of sampling point (20) pulse.

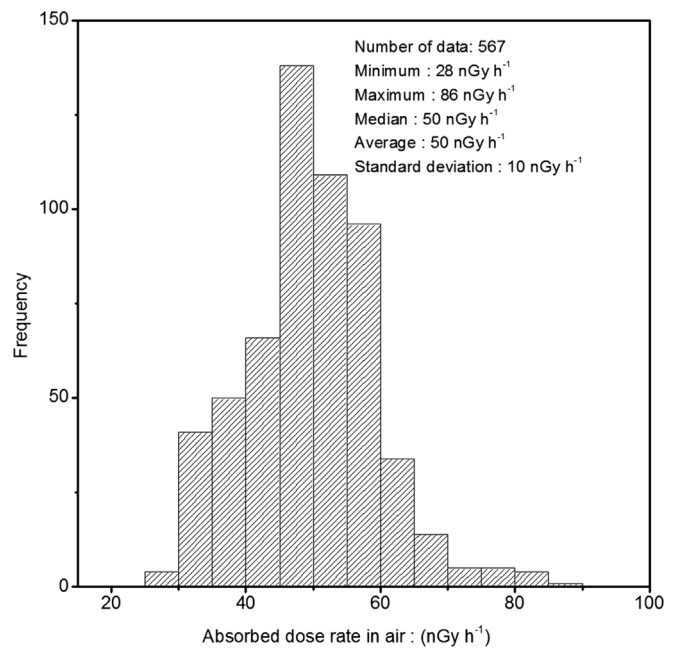


Fig. 7. Histogram of absorbed dose rate in air.

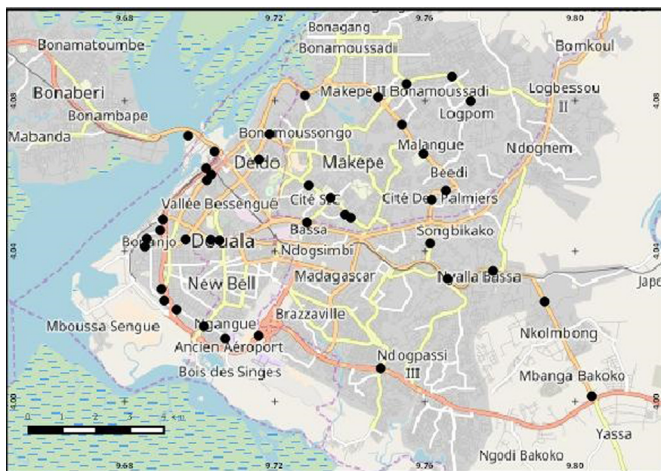


Fig. 6. *In situ* measurement points (39) of gamma-ray pulse height distribution using a NaI(Tl) scintillation spectrometer.

mean activity concentration of  $^{238}\text{U}$  is higher than the average value measured in other areas of Cameroon such as Bakassi and Poli, and lower than those measured in Lolodorf and Douala quarries. The same comparison can be made with those measured in Lagos state in Nigeria, Itagunmodi and Canakkale in Turkey, and in Kerala in India. For  $^{232}\text{Th}$ , the average activity concentration found out in the present study is higher than those of Bakassi and Poli, and lower than those measured at Douala-quarriers and Lolodorf. This value is also higher than those of Itagunmodi and Lagos State and lower than that of Kerala. The average value of  $^{40}\text{K}$

**Table 1.** *In situ* activity concentrations and the contributions of  $^{40}\text{K}$ ,  $^{238}\text{U}$  and  $^{232}\text{Th}$  to air absorbed dose rates in Douala using the car-borne survey method.

Point	Latitude	Longitude	Absorbed dose rate in air (nGy h <sup>-1</sup> )	Contribution to the dose rate (%)			Activity concentrations (Bq kg <sup>-1</sup> )		
	N	E		$^{40}\text{K}$	$^{238}\text{U}$	$^{232}\text{Th}$	$^{40}\text{K}$	$^{238}\text{U}$	$^{232}\text{Th}$
Douala	N4.05883	E9.701882	50 ± 1	12	28	60	146 ± 3	33 ± 2	48 ± 2
Douala	N4.060352	E9.703057	50 ± 1	23	25	53	292 ± 6	31 ± 2	44 ± 2
Douala	N4.062082	E9.701685	59 ± 1	27	33	40	386 ± 8	45 ± 3	36 ± 2
Douala	N4.06649	E9.703935	32 ± 1	34	24	40	290 ± 6	18 ± 1	21 ± 1
Douala	N4.070663	E9.696892	45 ± 1	36	23	41	410 ± 8	25 ± 3	30 ± 2
Douala	N4.048405	E9.690173	32 ± 1	23	23	53	185 ± 4	18 ± 1	27 ± 1
Douala	N4.045582	E9.689423	41 ± 1	17	28	54	187 ± 4	29 ± 2	37 ± 2
Douala	N4.043308	E9.685862	29 ± 1	15	28	57	110 ± 2	20 ± 1	28 ± 1
Douala	N4.041148	E9.685378	39 ± 1	12	30	58	129 ± 3	30 ± 2	39 ± 2
Douala	N4.029897	E9.68979	45 ± 1	16	26	59	184 ± 4	28 ± 2	44 ± 2
Douala	N4.026803	E9.690527	36 ± 1	14	26	60	130 ± 3	24 ± 2	36 ± 2
Douala	N4.024398	E9.693795	52 ± 1	13	30	58	177 ± 4	39 ± 3	51 ± 3
Douala	N4.019988	E9.701103	40 ± 1	20	26	55	210 ± 4	26 ± 2	37 ± 2
Douala	N4.016748	E9.706783	33 ± 1	16	29	55	146 ± 3	25 ± 2	32 ± 2
Douala	N4.05417	E9.734857	48 ± 1	16	25	58	208 ± 4	31 ± 2	47 ± 2
Douala	N4.057508	E9.729035	41 ± 1	23	26	51	246 ± 5	27 ± 2	35 ± 2
Douala	N4.064372	E9.715773	49 ± 1	15	29	56	200 ± 4	36 ± 3	47 ± 2
Douala	N4.071107	E9.718553	36 ± 1	23	26	52	208 ± 4	22 ± 2	31 ± 2
Douala	N4.081412	E9.728038	31 ± 1	16	29	56	131 ± 3	23 ± 2	30 ± 2
Douala	N4.080985	E9.747512	37 ± 1	13	27	60	124 ± 2	26 ± 2	38 ± 2
Douala	N4.084458	E9.755105	44 ± 1	13	29	59	143 ± 3	30 ± 2	42 ± 2
Douala	N4.086427	E9.767235	46 ± 1	23	21	56	286 ± 6	25 ± 2	44 ± 2
Douala	N4.079912	E9.772208	32 ± 1	15	28	57	130 ± 3	18 ± 1	32 ± 2
Douala	N4.073662	E9.753895	35 ± 1	13	28	59	125 ± 3	25 ± 2	36 ± 2
Douala	N4.065873	E9.759602	33 ± 1	16	27	57	139 ± 3	23 ± 2	32 ± 2
Douala	N4.056127	E9.765598	43 ± 1	15	25	61	167 ± 3	27 ± 2	44 ± 2
Douala	N4.053658	E9.761817	52 ± 1	15	25	61	201 ± 4	33 ± 2	54 ± 3
Douala	N4.042078	E9.761412	42 ± 1	16	24	59	176 ± 4	25 ± 2	42 ± 2
Douala	N4.032633	E9.766025	42 ± 1	22	25	53	237 ± 5	26 ± 2	37 ± 2
Douala	N4.03475	E9.778138	49 ± 1	15	25	60	194 ± 4	31 ± 2	50 ± 3
Douala	N4.026533	E9.791902	44 ± 1	16	25	60	184 ± 4	28 ± 2	45 ± 2
Douala	N4.00135	E9.804472	40 ± 1	22	24	54	223 ± 4	24 ± 2	36 ± 2
Douala	N4.049702	E9.738715	50 ± 1	24	25	51	312 ± 6	31 ± 2	43 ± 2
Douala	N4.048875	E9.740258	48 ± 1	16	25	59	200 ± 4	30 ± 2	47 ± 2
Douala	N4.047623	E9.728583	31 ± 1	20	27	54	155 ± 3	20 ± 1	28 ± 1
Douala	N4.04285	E9.705237	43 ± 1	20	44	36	231 ± 5	47 ± 3	26 ± 1
Douala	N4.043018	E9.702948	47 ± 1	29	33	39	359 ± 7	39 ± 3	31 ± 2
Douala	N4.043115	E9.696225	44 ± 1	17	35	48	197 ± 4	39 ± 3	36 ± 2
Douala	N4.017505	E9.715673	40 ± 1	12	36	52	127 ± 3	37 ± 3	36 ± 2

is higher than that is obtained in Bakassi and less than the average values found at Douala-quarriers, Lolodorf and Poli. Compared to other studies in the world, this value is higher than that of Canakkale, lower than those of Lagos state, Itagunmodi and Kerala. Figure 8 shows a weak correlation between thorium and uranium (correlation coefficient = 0.09).

The contributions of  $^{238}\text{U}$ ,  $^{232}\text{Th}$  and  $^{40}\text{K}$  to the absorbed dose rates in air range respectively between 21–44%, 36–61% and 12–36% with the average values of 27%, 54% and 19% respectively. The highest contributions of  $^{238}\text{U}$ ,  $^{232}\text{Th}$  and  $^{40}\text{K}$  to the absorbed dose rate were respectively found at Akwa (44%) (N4.04285, E9.705237), Beedi (61%) (N4.053658, E9.761817) and SCDP (36%) (N4.06649, E9.703935) while

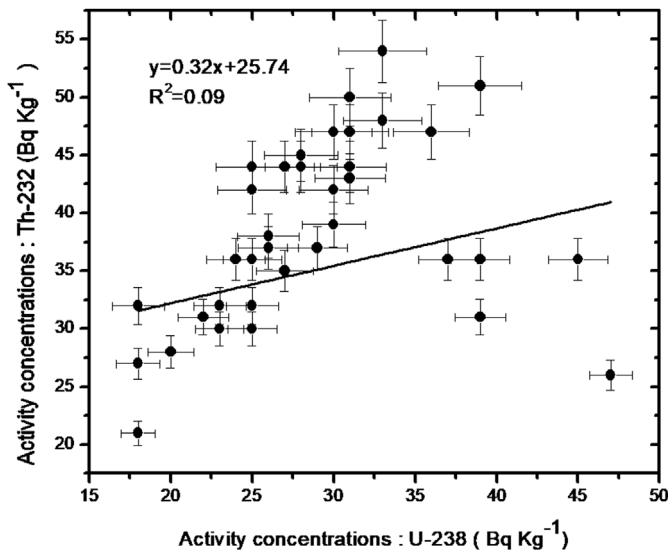


Fig. 8. Correlation between  $^{232}\text{Th}$  and  $^{238}\text{U}$  activity concentrations.

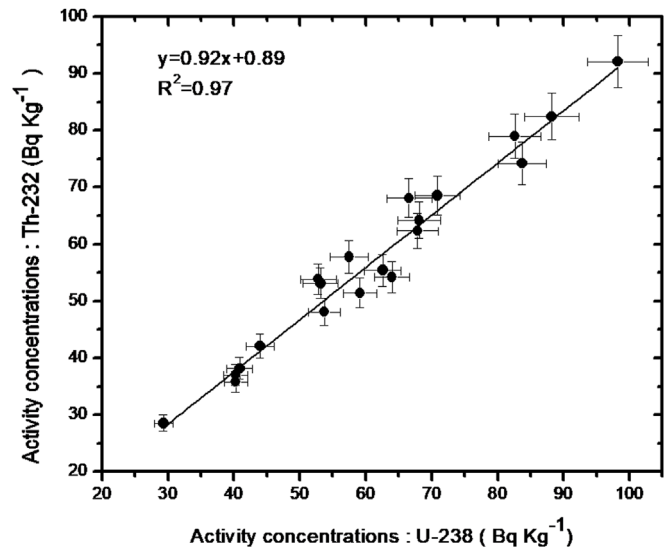


Fig. 9. Correlation between  $^{232}\text{Th}$  and  $^{238}\text{U}$  activity concentrations.

**Table 2.** Activity concentrations of  $^{238}\text{U}$ ,  $^{232}\text{Th}$  and  $^{40}\text{K}$  in soil, air absorbed dose rates and annual effective dose following radioactivity measurements at the laboratory.

Sample code	Location		Activity concentration ( $\text{Bq kg}^{-1}$ )			Absorbed dose rate	Annual effective dose
	Latitude	Longitude	$^{40}\text{K}$	$^{238}\text{U}$	$^{232}\text{Th}$	( $\text{nGy h}^{-1}$ )	( $\text{mSv y}^{-1}$ )
STN-16-39	04°01'640"	09°44'424"	40 ± 8	88 ± 17	82 ± 18	92 ± 13	0.6 ± 0.1
STN-16-40	04°01'625"	09°44'510"	41 ± 9	52 ± 10	53 ± 12	58 ± 9	0.4 ± 0.1
STN-16-41	04°01'642"	09°44'345"	43 ± 9	66 ± 13	64 ± 14	72 ± 10	0.5 ± 0.1
STN-16-42	04°01'395"	09°44'284"	53 ± 11	39 ± 08	37 ± 8	43 ± 6	0.3 ± 0 (<0.1)
STN-16-43	04°01'342"	09°44'240"	42 ± 9	52 ± 10	48 ± 11	55 ± 8	0.4 ± 0.1
STN-16-44	04°01'136"	09°44'239"	77 ± 16	29 ± 06	29 ± 6	34 ± 5	0.2 ± 0 (<0.1)
STN-16-45	04°00'995"	09°44'766"	44 ± 9	65 ± 13	68 ± 15	73 ± 11	0.5 ± 0.1
STN-16-46	04°00'907"	09°44'810"	47 ± 10	69 ± 14	69 ± 15	76 ± 11	0.5 ± 0.1
STN-16-47	04°00'835"	09°44'746"	60 ± 13	39 ± 08	36 ± 8	43 ± 6	0.3 ± 0 (<0.1)
STN-16-48	04°00'769"	09°44'619"	59 ± 13	52 ± 10	54 ± 12	59 ± 9	0.4 ± 0.1
STN-16-49	04°00'822"	09°44'595"	62 ± 13	43 ± 08	42 ± 9	48 ± 7	0.3 ± 0 (<0.1)
STN-16-50	04°00'861"	09°44'702"	43 ± 9	56 ± 11	58 ± 13	63 ± 9	0.4 ± 0.1
STN-16-51	04°01'047"	09°44'320"	51 ± 11	58 ± 11	51 ± 11	60 ± 8	0.4 ± 0.1
STN-16-52	04°01'016"	09°44'089"	64 ± 13	62 ± 12	54 ± 12	65 ± 9	0.4 ± 0.1
STN-16-53	04°01'258"	09°44'046"	74 ± 16	61 ± 12	55 ± 12	65 ± 9	0.4 ± 0.1
STN-16-54	04°01'302"	09°44'055"	67 ± 14	40 ± 08	38 ± 8	45 ± 6	0.3 ± 0 (<0.1)
STN-16-55	04°01'433"	09°44'016"	79 ± 17	66 ± 13	62 ± 14	72 ± 10	0.5 ± 0.1
STN-16-56	04°01'421"	09°43'763"	68 ± 14	82 ± 16	74 ± 16	86 ± 12	0.6 ± 0.1
STN-16-57	04°01'371"	09°43'740"	52 ± 11	81 ± 16	79 ± 17	88 ± 13	0.6 ± 0.1
STN-16-58	04°01'188"	09°43'941"	46 ± 10	96 ± 19	92 ± 20	102 ± 15	0.7 ± 0.1

the lowest contributions were found at Makepe (36%) (N4.04285, E9.705237) and Akwa (12%) (N4.017505, E9.715673) for  $^{232}\text{Th}$  and  $^{40}\text{K}$  respectively.

### 3.5 Activity concentrations of $^{238}\text{U}$ , $^{232}\text{Th}$ and $^{40}\text{K}$ in soil following laboratory measurements

Activity concentrations of natural radionuclides  $^{238}\text{U}$ ,  $^{232}\text{Th}$  and  $^{40}\text{K}$  in 20 soil samples using gamma spectrometry in laboratory are listed in Table 2. They range respectively

between 29–96  $\text{Bq kg}^{-1}$ , 29–92  $\text{Bq kg}^{-1}$ , and 40–79  $\text{Bq kg}^{-1}$  with respective average values of 60  $\text{Bq kg}^{-1}$ , 57  $\text{Bq kg}^{-1}$  and 56  $\text{Bq kg}^{-1}$ . The world average values of  $^{238}\text{U}$ ,  $^{232}\text{Th}$  and  $^{40}\text{K}$  in the earth's crust are 35, 30 and 400  $\text{Bq kg}^{-1}$ , respectively (UNSCEAR, 2000). It appears that average values of  $^{238}\text{U}$  and  $^{232}\text{Th}$  are higher than the corresponding world average activity concentrations. Figure 9 shows a good correlation between thorium and uranium in soil samples (correlation coefficient = 0.97). The highest  $^{238}\text{U}$  and  $^{232}\text{Th}$  activity concentrations were found at Brazzaville (96  $\text{Bq kg}^{-1}$ ), and

**Table 3.** Comparison of activity concentrations of  $^{238}\text{U}$ ,  $^{232}\text{Th}$  and  $^{40}\text{K}$  in soil samples from Douala littoral region following laboratory and *in situ* measurements with values from other areas around the world.

Country		Activity concentration (Bq kg <sup>-1</sup> )			References
		$^{238}\text{U}$	$^{232}\text{Th}$	$^{40}\text{K}$	
Nigeria	Lagos state	1.20–55.30(23)	2.18–60.33(23)	44.74–489.96(204)	Ojo and Gbadegesin (2015)
	Itangunmodi	18.5–90.3(55)	12.5–52.4(26)	200.5–901.2(501)	Ademola <i>et al.</i> (2014)
Turkey	Canakkale	14.9–118(42)	18.7–146(53)	197.1–1033.4(54)	Turhan <i>et al.</i> (2012)
India	Kerala	25–1269	42–2374	22–964	Hosoda <i>et al.</i> (2015)
Cameroon	Poli	12–57(24)	15–58(28)	112–1124(506)	Saïdou <i>et al.</i> (2015b)
	Bakassi	17–23(19)	27–38(32)	93–138(110)	Saïdou <i>et al.</i> (2015b)
	Lolodorf	60–270(130)	100–700(390)	370–1530(850)	Saïdou <i>et al.</i> (2015b)
	Douala (quarries)	11.8–146.7(40)	8–102.9(43)	54–928(342)	Guembou <i>et al.</i> (2017)
	Douala	<i>In situ</i>	18–47(29)	21–54(38)	110–410(202)
	Labo	29–96(60)	29–92(57)	40–79(56)	

( ): mean values.

Dakar for  $^{40}\text{K}$  (79 Bq kg<sup>-1</sup>) and the lowest activity concentrations of  $^{238}\text{U}$  and  $^{232}\text{Th}$  were found at Bilongue (29 Bq kg<sup>-1</sup>) and Oyack for  $^{40}\text{K}$  (40 Bq kg<sup>-1</sup>). The results of activity concentrations of natural radionuclides in soil samples taken from Douala III at different locations and in other parts of the world are displayed in Table 3. It clearly appears that activity concentrations of  $^{238}\text{U}$  and  $^{232}\text{Th}$  were higher than those of other areas in Cameroon (Bakassi, Poli and Douala-quarries), except Lolodorf and other countries (Lagos state, Itangunmodi, Canakkale).

The external terrestrial gamma radiation absorbed dose rates range between 34 and 102 nGy h<sup>-1</sup>, with an average value of 65 nGy h<sup>-1</sup>, which is higher than the world average value of 59 nGy h<sup>-1</sup> (UNSCEAR, 2000). According to Table 2, absorbed dose rates at 13 over 20 measurement points were higher than the world average value (59 nGy h<sup>-1</sup>). External effective dose of 8 over 20 measurement points is higher than the worldwide average value. The highest effective dose was found at Brazzaville (0.7 mSv y<sup>-1</sup>) and Oyack (0.6 mSv y<sup>-1</sup>). However, for *in situ* measurements, Table 1 shows that all measurement points have absorbed dose rate lower than the worldwide average value. External effective dose varies from 0.3–0.7 mSv y<sup>-1</sup> with an average value of 0.42 mSv y<sup>-1</sup>, which is lower than the worldwide average value (0.5 mSv y<sup>-1</sup>). The average value of the effective amount obtained in this study compared to other inhabited areas of Cameroun (Poli and Lolodorf) is low, and high in Bakassi (Saïdou *et al.*, 2015b).

## 4 Conclusion

The car-borne survey using NaI(Tl) scintillation spectrometer was carried out in Douala, the largest city of Cameroon to make the detailed distribution map of absorbed dose rate in air. Activity concentrations of  $^{238}\text{U}$ ,  $^{232}\text{Th}$  and  $^{40}\text{K}$  were also determined using *in situ* gamma spectrometry. They range respectively between 18–47 Bq kg<sup>-1</sup>, 21–54 Bq kg<sup>-1</sup> and 110–410 Bq kg<sup>-1</sup> with respective average values of 29 Bq kg<sup>-1</sup>, 38 Bq kg<sup>-1</sup> and 202 Bq kg<sup>-1</sup>. Mean activity concentrations of  $^{238}\text{U}$  and  $^{40}\text{K}$  are lower than the world average values

(UNSCEAR, 2000) while the mean activity concentration of  $^{232}\text{Th}$  is higher than the corresponding world average value. The contributions of  $^{238}\text{U}$ ,  $^{232}\text{Th}$  and  $^{40}\text{K}$  to the absorbed dose rates in air range respectively between 21–44%, 36–61% and 12–36% with the average values of 27%, 54% and 19%. The average activity concentrations of natural radionuclides  $^{238}\text{U}$ ,  $^{232}\text{Th}$  and  $^{40}\text{K}$  in the soil were found to be 60 Bq kg<sup>-1</sup>, 57 Bq kg<sup>-1</sup> and 56 Bq kg<sup>-1</sup> respectively. The total average effective dose is 0.37 mSv y<sup>-1</sup> which is lower than the worldwide average value (0.5 mSv y<sup>-1</sup>). Finally, it can be concluded that the population of Douala city is not significantly exposed to natural radiation.

## References

- Ademola KA, Bello KA, Adejumbi CA. 2014. Determination of natural radioactivity and hazard in soil samples in and around gold mining area in Itangunmodi, south-western, Nigeria. *J. Radiat. Res. Appl. Sci.* 7: 249–255.
- Beck HL. 1972. *The absolute intensities of gamma rays from the decay of  $^{238}\text{U}$  and  $^{232}\text{Th}$* . Health and Safety Laboratory Report HASL-262. New York: U.S. Atomic Energy Commission.
- Beck HL, DeCampo J, Gogolak C. 1972. *In-situ Ge(Li) and NaI(Tl) gamma-ray spectrometry*. Health and Safety Laboratory Report HASL-258. New York: U.S. Atomic Energy Commission.
- EPA. 2009. Sources of background radioactivity. <http://www.epa.gov/radiation/marsim/docs/marsame/appendix.B.pdf>. Accessed 9 August 2011.
- Guembou Shouop SJ, Ndontchueng Moyo M, Chene G, Nguelem Mekontso EJ, Motapon Ousmanou, Kayo AS, Strivay D. 2017. Assessment of natural radioactivity and associated radiation hazards in sand building material used in Douala Littoral Region of Cameroon using gamma spectrometry. *Environ. Earth Sci.* 76: 1–12.
- Hosoda M, Tokonami S, Omori Y, Sahoo SK, Akiba S, Sorimachi A, Ishikawa T, Nair RR, Jayalekshmi PA, Sebastian P, Iwaoka K, Akata N, Kudo H. 2015. Estimation of external dose by car-borne survey in Kerala, India. *Plos ONE* 10: e0124433.
- Hosoda M, Inoue K, Oka M, Omori Y, Iwaoka K, Tokonami S. 2016. Environmental radiation monitoring and external dose estimation

- in Aomori prefecture after the Fukushima Daiichi Nuclear Power Plant accident. *Jpn. J. Health Phys.* 51: 41–50.
- IAEA. 1989. Measurement of radionuclides in food and the environment, a guidebook. International Atomic Energy Agency Technical Reports Series No. 229, Vienna.
- Inoue K, Hosoda M, Fukushi M, Furukawa M, Tokonami S. 2015. Absorbed dose rate in air in metropolitan Tokyo before the Fukushima Daiichi Nuclear Power Plant accident. *Radiat. Prot. Dosim.* 167: 231–234.
- Inoue K, Arai M, Fujisawa M, Saito K, Fukushi M. 2017. Detailed distribution map of absorbed dose rate in air in Tokatsu area of Chiba prefecture, Japan, constructed by car-borne survey 4 years after the Fukushima Daiichi Nuclear Power Plant accident. *Plos ONE* 12: e0171100.
- Jacob P, Paretzke HG, Rosenbaum H, Zankl M. 1986. Effective dose equivalents for photon exposure from plane sources on the ground. *Radiat. Prot. Dosim.* 14: 299–310.
- JCGM 100. 2008. Joint Committee for Guides in Metrology. Evaluation of measurement data-guide to the expression of uncertainty in measurement, September 2008. [http://www.bipm.org/utis/common/documents/jcgm/JCGM\\_100\\_2008\\_E.pdf](http://www.bipm.org/utis/common/documents/jcgm/JCGM_100_2008_E.pdf). Accessed 19 August 2016.
- Kocher DC, Sjoreen AL. 1985. Dose-rate conversion factors for external exposure to photon emitters in soil. *Health Phys.* 48: 193–205.
- Leung KC, Lau SY, Poon CB. 1990. Gamma radiation dose from radionuclides in Hong Kong soil. *J. Environ. Radioact.* 11: 279–290.
- Matsuda H, Furukawa S, Kaminishi T, Minato S. 1982. A new method for evaluating weak leakage gamma-ray dose using a 3"φ × 3" NaI (TI) scintillation spectrometer (I) Principle of background estimation method. Rep Government Industrial Research Institute. *Nagoya* 31: 132–146. In Japanese.
- Matsuda H, Minato S, Pasquale V. 2002. Evaluation of accuracy of response matrix method for environmental gamma ray analysis. *Radioisotopes* 51: 42–50. In Japanese.
- Minato S. 1971. Terrestrial gamma-radiation field in natural environment. *J. Nucl. Sci. Technol.* 8: 342–347.
- Minato S. 1977. Analysis of the variation of environmental  $\gamma$  radiation during rainfall. Rep Government Industrial Research Institute. *Nagoya* 26: 190–202. In Japanese.
- Minato S. 1978. A response matrix of a 3"φ × 3" NaI(Tl) scintillator for environmental gamma radiation analysis. Rep Governmental Industrial Research Institute. *Nagoya* 27: 384–397. In Japanese.
- Minato S. 1980. Monte Carlo calculation of gamma radiation field due to precipitation washout of radon daughters from the atmosphere to the ground surface. *Jpn. J. Health Phys.* 15: 19–24.
- Minato S. 2001. Diagonal elements fitting technique to improve response matrixes for environmental gamma ray spectrum unfolding. *Radioisotopes* 50: 463–471.
- Minato S. 2012. Application of a 60 × 60 response matrix for a NaI (TI) Scintillator to fallout from the Fukushima reactor accident. *Radiat. Emerg. Med.* 1: 108–112.
- Minato S, Kawano M. 1970. Evaluation of exposure due to terrestrial gamma-radiation by response matrix method. *J. Nucl. Sci. Technol.* 7: 401–406.
- Moriuchi S, Tsutsumi M, Saito K. 1990. Examination on conversion factors to estimate effective dose equivalent from absorbed dose in air for natural gamma radiations. *Jpn. J. Health Phys.* 25: 121–128. Japanese with English abstract.
- Ndoutchueng MM, Njinga RL, Nguelem EJM, Simo A, Beyala Ateba JF. 2014. <sup>238</sup>U, <sup>235</sup>U, <sup>137</sup>Cs and <sup>133</sup>Xe in soils from two campuses in University of Douala-Cameroon. *Appl. Radiat. Isot.* 86: 85–89.
- Ngoa EL, Ndjana NJE, Hosoda M, Bongue D, Saïdou, Akata N, Koukoug HR, Kwato NMG, Tokonami S. 2017. Air absorbed dose rate measurements and external dose assessment by car-borne survey in the gold mining areas of Betare-Oya, Eastern-Cameroon. *Jpn. J. Health Phys.* 53: 5–11.
- Ojo TJ, Gbadegesin KAJ. 2015. Terrestrial radiation doses from selected towns of Southwestern Nigeria. *Int. J. Phys.* 3: 244–247.
- Olivry CJ. 1986. Fleuves et rivières du Cameroun. Collection Monographies Hydrologiques. Paris: ORSTOM, n° 9.
- Ravisankar R, Vanasundari K, Chandrasekaran A, Suganya M, Eswaran P, Vijayagopal P, Meenakshisundaram V. 2011. Measurement of natural radioactivity in brick samples of Namakkal, Tamilnadu, India using gamma ray spectrometry. *Arch. Phys. Res.* 2: 95–99.
- Saïdou, Abdourahimi, Tchuenta Siaka YF, Kwato Njock MG. 2015a. Natural radiation exposure to the public in the oil bearing Bakassi Peninsula, Cameroon. *Radioprotection* 50(1): 35–41.
- Saïdou, Ele Abiama P, Tokonami S. 2015b. Comparative study of natural radiation exposure to the public in three uranium and oil regions of Cameroon. *Radioprotection* 50(4): 265–271.
- Tan VL, Inoue K, Fujisawa M, Arai M, Fukushi M. 2017. Impact on absorbed dose rate in air from Asphalt Pavement Associated with Transport Infrastructure Developments on Phu Quoc Island, Vietnam. *Radiat. Environ. Med.* 2: 88–93.
- Turhan S, Arkan IH, Oguz F, Özdemir T, Yücel B, Varinlioglu A, Köse A. 2012. Car-borne survey of natural background gamma dose rate in Çanakkale region, Turkey. *Radiat. Prot. Dosim.* 148: 45–50.
- UNSCEAR. 1982. Ionizing radiation sources and biological effects. United Nations, New York.
- UNSCEAR. 2000. Report to the general assembly, with scientific annexes. Annex B exposures from natural radiation sources. New York Report of the United Nations Scientific.

**Cite this article as:** Takoukam Soh SD, Saïdou, Hosoda M, Ndjana Nkoulou II JE, Akata N, Bouba O, Tokonami S. 2018. Natural radioactivity measurements and external dose estimation by car-borne survey in Douala city, Cameroon. *Radioprotection* 53(4): 255–263